ResearchGate

See discussions, stats, and author profiles for this publication at: https://www.researchgate.net/publication/13730502

# Thermal analysis of freeze-dried liposome-carbohydrate mixtures with modulated temperature differential scanning calorimetry

**ARTICLE** *in* JOURNAL OF PHARMACEUTICAL SCIENCES · MARCH 1998

Impact Factor: 2.59 · DOI: 10.1021/js970060b · Source: PubMed

CITATIONS
24

READS
21

**3 AUTHORS:**

Ewoud van Winden
Medochemie Ltd
**12** PUBLICATIONS **228** CITATIONS
SEE PROFILE

Herre Talsma
Utrecht University
**91** PUBLICATIONS **3,002** CITATIONS
SEE PROFILE

Daan Crommelin
Utrecht University
**405** PUBLICATIONS **12,210** CITATIONS
SEE PROFILE

Available from: Herre Talsma
Retrieved on: 02 February 2016

# Thermal Analysis of Freeze-Dried Liposome–Carbohydrate Mixtures with Modulated Temperature Differential Scanning Calorimetry

E. C. A. VAN WINDEN*, H. TALSMA, AND D. J. A. CROMMELIN

Contribution from *the Department of Pharmaceutics, Utrecht Institute for Pharmaceutical Sciences (UIPS),*† *Utrecht University, Utrecht, The Netherlands*

Received February 10, 1997. Accepted for publication November 4, 1997.

**Abstract** □ In this study we investigated the use of modulated temperature differential scanning calorimetry (MTDSC) for the detection of the glass transition temperature ($T_g$) in freeze-dried cakes of lyoprotected liposomes and for the analysis of frozen carbohydrate solutions. The glass transition appeared in the reversing heat flow, whereas the bilayer melting endotherm was observed in the nonreversing heat flow. This enabled the detection of $T_g$ even in samples were the glass and bilayer transition overlapped. In addition, relaxation processes occurring in nonannealed freeze-dried carbohydrate–liposome mixtures, which hinder the determination of $T_g$ with conventional DSC, were also separated from the heat capacity related heat flow. Analysis of frozen carbohydrate solutions with MTDSC facilitated the identification of the glass transition, devitrification peak, and "softening" transition, which could help to further optimize freeze-drying conditions by rationale. Sampling and selection of experimental parameters are discussed for the special case of porous, freeze-dried cakes.

## Introduction

Freeze-drying is a frequently used technique to improve the stability for systems which are labile in an aqueous environment, such as certain proteins and liposomes. Carbohydrates are often added for protection against dehydration stress (lyoprotection), which results in a solid, amorphous matrix around the liposomes or proteins after drying. The stability of such dried systems is the subject of a growing number of investigations, especially for lyoprotected proteins.[1−6] The glass transition temperature ($T_g$) of the sugar matrix is considered to be a critical parameter regarding the long-term stability of the dried protein. Generally, slow chemical and physical degradation is observed in the glassy phase at temperatures below $T_g$, because of the low molecular mobility. In the less viscous phase above $T_g$, these processes are strongly accelerated.

In principle, the $T_g$ can be observed as a change in heat capacity with differential scanning calorimetry (DSC),[3,7−9] but in stability studies it is often difficult to detect the glass transition when other thermal events occur in the same temperature range. Recently, a novel extension of DSC, modulated temperature DSC (MTDSC), has been developed.[10−14] With this technique a heat capacity related heat flow can be distinguished from the total heat flow, facilitating the identification of the glass transition and the determination of $T_g$. Recently, Coleman and Craig[15] reviewed the current literature on the application of MTDSC for the analysis of pharmaceutical systems. In this study we investigated the use of MTDSC for the detection of $T_g$ in freeze-dried, lyoprotected liposomes, an important parameter for shelf-life stability,[16] and in the freeze-concentrate of carbohydrate solutions, to rationalize the freeze-drying process. For this purpose, we compared MTDSC heating profiles with those obtained by conventional DSC as described in this study and by others (e.g. refs 17−20). MTDSC analyses of formulations with different carbohydrates and lipid compositions, with and without encapsulated drug, were tested to demonstrate the versatility of this technique. Doxorubicin (DXR) was selected as a model drug for the encapsulation into liposomes, since DXR liposomes can be considered potential candidates for extension of shelf-life stability by freeze-drying. The pH for optimal stability of phospholipids and doxorubicin in an aqueous environment are different, pH 6.5 and about pH 4, respectively.[21,22] Therefore, the stability of freeze-dried doxorubicin liposomes has been the subject of investigation in our group.[23]

**Modulated Temperature DSC**—For a proper interpretation of the potential value of MTDSC, a basic understanding of the principle behind this technique is required. A detailed description of MTDSC has been published elsewhere.[10,11,13,14] The main principles can be summarized as follows.

With conventional DSC, the sample is subjected to a constant heating rate. The registered heat flow to increase the sample temperature may be divided into two components, one depending on the heat capacity of the sample and the other depending on thermally activated or kinetically driven processes occurring in the sample. Only the first component which is related to the heat capacity depends proportionally on the heating rate. This difference is exploited in MTDSC.

With MTDSC, a small sinusoidal temperature modulation [characterized by a period ($p$) and temperature amplitude ($T_a$)] is superimposed on the constant heating rate ($q$) of the furnace plate. This modulation is followed by the sample with a small phase lag. As a consequence, the heating rate of the sample is modulated, which also results in a sinusoidal modulation of the required heat flow to the sample. Within a narrow temperature range, the difference in the heat flows at the average and maximum heating rate will only depend on the heat capacity of the sample. The average heat flow, however, depends on both the heat capacity and all thermal events in the sample which occur at that temperature. In other words, only a change in heat capacity during the scan will be reflected as a change in the amplitude of the modulated heat flow, whereas all thermal events will become visible in the average heat flow. The average heat flow equals the signal observed with conventional DSC and is called the "total" heat flow.

During the scan, the amplitude of the modulated heat flow is determined by Fourier transform deconvolution. The

* Corresponding author. Current address: OctoPlus B. V., PO Box 722, 2300 AS, Leiden, The Netherlands. Phone, +31 71 5680268; fax, +31 71 5234144.

† Participant in the research school Groningen Utrecht Institute for Drug Exploration (GUIDE).

© 1998, American Chemical Society and American Pharmaceutical Association

S0022-3549(97)00060-9 CCC: $15.00 Published on Web 01/16/1998

heat capacity is calculated by division of the heat flow amplitude by the sample weight and the heating rate amplitude (eq 1). The heat flow correlated with the heat capacity ($C_p$) is then calculated by multiplying the heat capacity with the average heating rate (eq 2). This is called the "reversing heat flow". The difference between the reversing and the total heat flow is called the "nonreversing" heat flow (eq 3). However, not all processes collectively described in this signal are irreversible (e.g. melting processes).

$$C_p(\text{J/g °C}) = \frac{\text{heat flow amplitude (J/s)}}{\text{heating rate amplitude (°C/s)} \times \text{sample weight (g)}} \quad (1)$$

$$\text{reversing heat flow [J/s g]} = C_p[\text{J/g °C}] \times \text{average heating rate (°C/s)} \quad (2)$$

$$\text{nonreversing heat flow} = \text{total heat flow} - \text{reversing heat flow} \quad (3)$$

## Experimental Section

**Materials**—Dipalmitoylphosphatidylcholine (DPPC), dipalmitoylphosphatidylglycerol (DPPG) were gifts from Nattermann Phospholipid GmbH (Köln, Germany). Cholesterol (CHOL) was obtained from Sigma Chemical Co. (St. Louis, MO). Doxorubicin (DXR) was a gift from Pharmachemie b.v. (Haarlem, The Netherlands). All other chemicals were of analytical grade and used without further purification. All aqueous solutions were prepared with water purified by reversed osmosis.

**Preparation of Liposomes**—Lipids were dissolved in a mixture of chloroform and methanol in a round-bottom flask. The solvent was removed by rotary evaporation at 40−45 °C and nitrogen was blown into the flask for 0.5 h. The lipids were hydrated at 50−60 °C with solutions containing 10% (w/v) carbohydrate and 10 mM Hepes (pH 7.4) as indicated under results. For DPPC liposomes 1 mM EDTA was added to the medium in order to minimize aggregation. The dispersions were extruded several times at elevated temperatures through polycarbonate membranes with pore sizes of 0.2, 0.1, and 0.05 $\mu$m (Unipore, Bio-Rad, Richmond, CA) until the desired vesicle size had been achieved.

Doxorubicin liposomes were prepared by the remote loading method[24] with some modifications.[23] Then, lipids were hydrated with 5% (w/v) disaccharide solutions containing 120 mM $(NH_4)_2SO_4$, followed by replacement of the extraliposomal medium by a 15% (w/v) carbohydrate, 10 mM Hepes (pH 7.4) solution using gel permeation chromatography. Doxorubicin was added to the extraliposomal medium at 60 °C and after loading and cooling the nonencapsulated drug was removed by addition of the cation-exchange resin Dowex 50WX-4[25] and subsequent filtration.

**Particle Size Determination**—Samples of the dispersion were diluted with 10% or 15% (w/v) sucrose containing 10 mM Hepes, pH 7.4, buffer. The average size and polydispersity was determined at 25 °C by dynamic light scattering with a Malvern 4700 system, using the automeasure version 3.2 software (Malvern Ltd, Malvern, UK). Mass distribution of the vesicle size is reported. The values of the viscosity and refractive index used in the calculation of the particle size of the light scattering data were 1.1713 g/m s and 1.348 for the 10% sucrose solution, respectively, and 1.3786 g/m s and 1.3549 for the 15% sucrose solution, respectively. The measured average size measurements of 100 nm standard particles (Polymer Laboratories Ltd., Shropshire, UK) deviated less than 5% from the size indicated by the manufacturer.

**Freeze-Drying of Liposomes**—Freshly prepared liposome dispersions were either stored at 4 °C until use or freeze-dried in aliquots of 0.4 mL in 13.5 mL freeze-dry vials. The rubber freeze-dry caps (type V9172-FM 257, Helvoet Pharma, Alken, Belgium) were dried at 100 °C for 1 day prior to use. The vials were frozen in boiling nitrogen for 10 min and placed on the freeze-dryer plate with a temperature of −40 °C. In the first step of the freeze-drying process, the plate temperature was maintained at −40 °C and the chamber pressure at 10−13 Pa for 30 h, followed by additional drying steps at plate temperatures of −30, −16, and +20 °C, each for 5 h at a pressure of ca. 1 Pa. The condenser temperature ranged between −55 and −60 °C. At the end of the freeze-drying process the chamber was filled with nitrogen, and the vials were closed with rubber caps and stored at 4 °C until further treatment.

**Residual Water Content**—The residual water content was determined with the Karl Fischer method using a Mitsubishi moisture meter model CA-05 (Tokyo, Japan). To minimize exposure of the hygroscopic cakes to the environment, the rubber caps remained on the vials throughout the sampling procedure. The pressure inside/outside the vials was equalized via a needle through the rubber caps before weighing the closed vials containing the cakes. Cakes were dissolved in 1 mL of Hydranal Coulomat A (Riedel de Haen, Seelze, Germany) which was injected through the rubber caps, allowing the release of overpressure through a second needle. The water content of 100 $\mu$L aliquots of the solvent was measured in duplicate. The weight of each empty vial was determined before usage, as was the weight of each used cap after cleaning and drying. Thus, the weight percentage of water in the freeze-dried cakes could be calculated.

**Phosphate Determination**—Lipid phosphate was determined by the colorimetric method of Rouser et al.[26]

**MTDSC Analysis**—To minimize attraction of water by the hygroscopic samples, sampling was performed in a dry nitrogen gas environment, and the time in which the cakes were exposed to these conditions was less than 2 min. Samples (2.5−5 mg) of the freeze-dried cakes were punched out and transferred into aluminum pans, which were sealed immediately. This sampling procedure resulted in a slight compression of the porous cakes. All scans were recorded with a DSC 2920 (TA Instruments, Inc., New Castle, DE), equipped with a liquid nitrogen cooling accessory. For a two-point temperature calibration indium and gallium were used as a standard. The heat capacity calibration constant was determined with a 62 mg sapphire disk as a standard, with $p = 100$ s and temperature modulation amplitude ($T_a$) = 0.159 °C at 30 °C. Scans were recorded under "heating only" conditions with 1 modulation/°C using the following settings: $q = 1$ °C/min, $p = 60$ s, $T_a = 0.159$ °C, or $q = 2$ °C/min, $p = 30$ s, $T_a = 0.159$ °C. The Thermal Analyst software version 8.6 was used for data evaluation. The $T_g$ values were determined by taking the half-height between the baseline below and above the temperature range of the glass transition. Sometimes, different heat flows of a sample were plotted on the same $y$-axis without data manipulation, but the position of the curves was adjusted for clarity reasons.

## Results and Discussion

**Sampling**—In this study the application of MTDSC for the analysis of freeze-dried liposome−carbohydrate mixtures is described. For the selected phospholipid bilayers, two major phase transitions are expected to occur in such cakes: the glass transition of the amorphous sugar and the main bilayer transition. Both transitions are influenced by the presence of water. As freeze-dried sugar cakes are hygroscopic and generally have a large surface area, adequate measures have to be taken to avoid exchange of water after finishing the drying procedure. Therefore, we performed all critical manipulations with the cakes in a dry cabinet. Although an increase in residual water content of the dry cakes as a function of exposure time to the sampling conditions was observed (data not shown), changes in residual water content of the 0.4 mL cakes within the short sampling time of 2 min were negligible as compared to the variability regarding residual water between the vials after freeze-drying. Before opening, the vials contained 0.21 ± 0.07% water (average ± SE, $n$ = 26, range 0.07−0.34%). After sampling, a residual water content of 0.26 ± 0.06% ($n$ = 10, range 0.19−0.35%) was measured.

**Selection of Experimental Parameters**—MTDSC requires a careful selection of the scanning parameters. First of all, for a proper heat capacity measurement, the temperature gradient in the sample should be negligible.

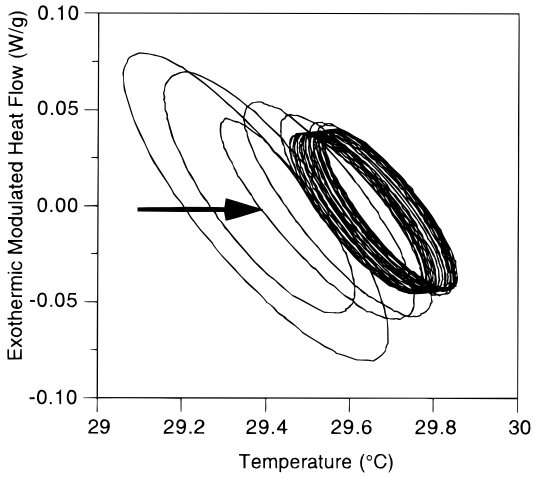


**Figure 1**—Modulated heat flow as a function of the modulated temperature in a quasi-isothermal analysis of freeze-dried, lyoprotected DPPC liposomes. Liposomal medium, 10% trehalose, 1 mM EDTA, and 10 mM Hepes, pH 7.4. The $T_a$ was set at 0.159 °C, $p$ at 30 s; sample weight, 4.3 mg; carbohydrate/phospholipid ratio, 3 g/g. Further information is provided in the text.

If part of the sample does not follow the heating rate modulation, the sample heat capacity is underestimated. A second requirement, which is related to the first one, is the existence of a linear response between the modulated heating rate and the modulated heat flow at constant heat capacity of the sample. In addition, at least four to six modulations over the temperature range of the transition are recommended to obtain good separation between thermal events which depend on heating rate and kinetically driven or thermally activated processes.

Increasing the temperature modulation amplitude ($T_a$) and the sample weight increases the sensitivity. However, a high-modulation frequency, a large amplitude, and a large sample size may lead to temperature gradients within the sample. The occurrence of these undesired temperature gradients also depends on the average heating rate and the heat conductivity of the sample. As freeze-dried cakes are porous, the expected poor heat conductivity of our samples required special attention to select the appropriate experimental conditions. A standard procedure to improve the heat conductivity of a sample is the exertion of high pressure to decrease sample volume and to increase the contact area between the sample and the aluminum pan. However, no such forces were applied to our samples to exclude possible physical changes induced by this protocol. In our experiments "heating only" conditions were maintained during the heating scans, and the maximal heating rate was 4 °C/min (average heating rate, 2 °C/min; amplitude, 0.159 °C; period, 30 s). The amplitude of 0.159 °C was found to result in an acceptable signal/noise ratio for the determination of $T_g$ in freeze-dried cakes of 2.5−5 mg.

In Figure 1, a Lissajous graph is shown in which the modulated heat flow in a quasi-isothermal measurement is plotted as a function of the temperature fluctuation. In this type of experiment, the sample undergoes a heating/cooling modulation. When equilibrium conditions exist in the sample during this modulation, the curve has the shape of a smooth ellipse which indicates the linear response between the heat flow and the temperature during all phases of the modulation. During this measurement the average temperature had not completely stabilized yet, resulting in a small gradual shift of the ellipse.

The absence of a temperature gradient can be verified by varying the period of the modulation. When an increase in the period does not result in an increase in observed

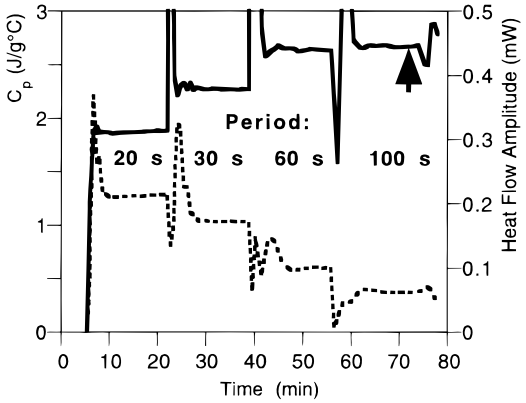


**Figure 2**—Heat capacity (—) and heat flow amplitude (– –) as a function of time, measured with different modulation frequencies ($p$). The $T_a$ was set at 0.159 °C throughout the experiment and stabilized within 10 min after a change in the modulation period. The average temperature ranged between 29.3 and 29.7 °C. See Figure 1 for sample description.

heat capacity, the total sample closely follows the furnace temperature pattern. This experiment is most easily done under quasi-isothermal conditions (constant average temperature), excluding temperature dependent changes in the heat capacity. Figure 2 displays the results of such a measurement of DPPC liposomes freeze-dried with trehalose (sample weight, 4.3 mg). From this figure, it is clear that quasi-isothermal modulation with $T_a$ = 0.159 °C resulted in an underestimation of the heat capacity when applying periods of 20 and 30 s. It appeared from these results that a good linear response of the modulated heat flow to the modulated temperature (smooth ellipse shape in Lissajous plot, $p$ = 30 s, $T_a$ = 0.159 °C, Figure 1) does not exclude the existence of a temperature gradient in the sample under the same experimental conditions (Figure 2). No difference was found between the heat capacity measured with periods of 60 and 100 s, indicating that under those conditions, no temperature gradient existed in the sample.

With an increasing modulation period, the maximal heating rate during the modulation is decreased, resulting in a smaller heat flow amplitude (Figure 2). Additional data sets of heat flows under quasi-isothermal conditions were collected and compared to a heating scan. Heating scans with a period of 30 s and an average heating rate of 2 °C/min (heating only conditions) gave the same heat capacity values as with $p$ = 100 s under quasi-isothermal conditions, as discussed below (see Figure 6).

**Standard DSC**—The determination of $T_g$ in freeze-dried sugar cakes by standard DSC is often hindered by other thermal processes in the sample (partly) occurring in the same temperature range. An example of repeated (standard) DSC scans of a freeze-dried solution of 15% (w/v) sucrose and 10 mM Hepes (pH 7.4) is given in Figure 3A. The origin of the thermal effect observed in the first scan is not clear to us. These processes are poorly reproducible. They may be artifacts or indicate metastability of the freeze-dried cakes. For unknown reasons, such processes were hardly observed in trehalose cakes indicating that it is unlikely that they result from sampling artifacts only. From Figure 3A it is clear that the sample has changed after the first scan, resulting in a relatively straight baseline and a clearly identifiable glass transition in the three subsequent scans. It is common practice that samples are annealed above their $T_g$ to allow the determination of $T_g$ with standard DSC. However, such annealing processes can induce significant physical changes to freeze-dried liposome−carbohydrate mixtures, such as a reduction in the bilayer transition temperature, as reported previ-

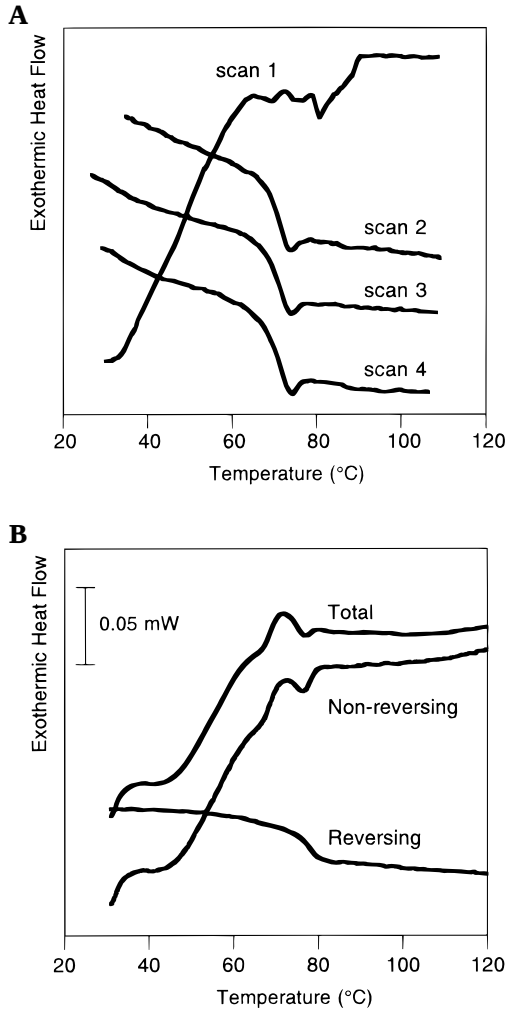


**Figure 3**—(A) Repeated DSC scans of freeze-dried solution containing 10% sucrose, 10 mM Hepes, pH 7.4; $q = 1$ °C/min. (B) MTDSC scan 1 of freeze-dried DXR liposomes with an extraliposomal medium containing 15% sucrose and 10 mM Hepes, pH 7.4. Lipid composition, DPPC:DPPG:CHOL = 10:1:4; $q = 1$ °C/min; $T_a = 0.159$ °C; $p = 60$ s; carbohydrate/phospholipid ratio, 4.4 g/g.

ously.[17,18] Therefore, information on the physical state of lyoprotected liposomes after freeze-drying can only be obtained in the first scan, which creates the need for detection of $T_g$ in the first scan as well.

In Figure 3B we demonstrate that this is possible with MTDSC for doxorubicin (DXR) containing DPPC:DPPG:CHOL = 10:1:4 liposomes freeze-dried in sucrose. These liposomes show a high retention of this cytostatic after a freeze-drying/rehydration cycle and were subjected to a solid-state stability study in our lab.[23] The presence of CHOL abolishes the bilayer transition in aqueous dispersions (data not shown), and therefore no clear melting behavior was expected in these samples. Scan 1 of the total heat flow shows again a pronounced thermal effect, which interferes with the identification of the glass transition, whereas $T_g$ can clearly be determined from the reversing heat flow of the same scan. Full separation was obtained between heat capacity related thermal events and other processes.

**Comparison between Total Heat Flow Derived from Standard and Modulated Temperature DSC**—A similar experiment was done with DXR liposomes freeze-dried in lactose in which the total heat flows obtained by standard DSC and MTDSC (same instrument, different operational mode) were compared (Figure 4). As demonstrated in Figure 3A, a proper comparison between the total heat flows from repeated scans of the same sample can only be made between scan 2 and subsequent scans. Scan 3, recorded with a constant heating rate, was identical with scan 2 (modulated heating rate), apart from a slightly higher noise level in the heat profile recorded with standard DSC. This illustrates that the total heat flow observed with MTDSC is nearly identical with the heat flow registered by standard DSC. The modulated heat flow depicted in Figure 4 (curve 1A) clearly demonstrates the increase in heat flow amplitude when heating the sample through its glass transition.

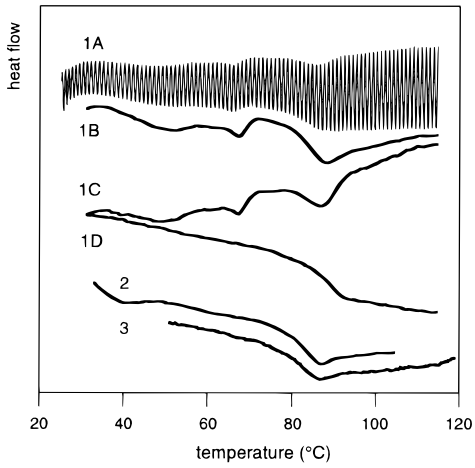


**Figure 4**—Scans 1, 2 (MTDSC), and 3 (DSC) of freeze-dried DXR liposomes with an extraliposomal medium containing 15% lactose and 10 mM Hepes, pH 7.4. The heat flow values of curve 1A were divided by a factor 2 for clarity reasons. Lipid composition, DPPC:DPPG:CHOL = 10:1:4; $q = 1$ °C/min; $T_a = 0.159$ °C; $p = 60$ s; carbohydrate/phospholipid ratio, 4.4 g/g. Scan 1: 1A, modulated heat flow; 1B, total heat flow; 1C, nonreversing heat flow, 1D reversing heat flow. Scan 2: total heat flow (MTDSC). Scan 3: conventional DSC.

**Differences in $T_g$ Assessment on the Basis of Total and Reversing Heat Flow Data**—A small difference in $T_g$ values was observed when this parameter was determined from the total heat flow (as with conventional DSC) or from the reversing heat flow as obtained with MTDSC. Close inspection of the shift in baseline in the total and reversing heat flow showed that the onset temperature for the glass transition ($T_{g,onset}$) in the total heat flow coincides with the relaxation peak in the nonreversing heat flow, whereas $T_{g,onset}$ in the reversing heat flow was found at slightly higher temperatures. For DXR liposomes freeze-dried in sucrose to residual water contents of 3.5 ± 0.2% and 0.4 ± 0.2% ($n = 10$), respectively, the $T_{g,onset}$ values obtained from these two heat flow recordings (total vs reversing heat flow) indeed differed with 3.2 ± 1.4 °C (average ± SD, $n = 13$, paired observations) and 3.7 ± 0.8 °C ($n = 17$), respectively. Apparently, the $T_{g,onset}$ in the total heat flow is a reflection of an endothermic relaxation process which is associated with the glass transition, but is not correlated with a change in heat capacity of the sample. However, differences in $T_{g,onset}$ determined from the total or reversing heat flow are small relative to the variability of $T_g$ values between different cakes and samples. The average $T_g$ value of the sucrose cakes with 3.5% residual water was 33 ± 5 °C in a range of 23−41 °C ($n = 14$), and 69 ± 4 °C ([62−74 °C], $n = 19$) in cakes containing 0.4% water. Analysis of the sum of squares showed that about 40% of the total variability could be ascribed to variation between samples taken from the same vials. These data reveal that despite the carefully designed sample handling protocol, a major source of variability in $T_g$ data can be found in (1) the sampling procedure, (2) the

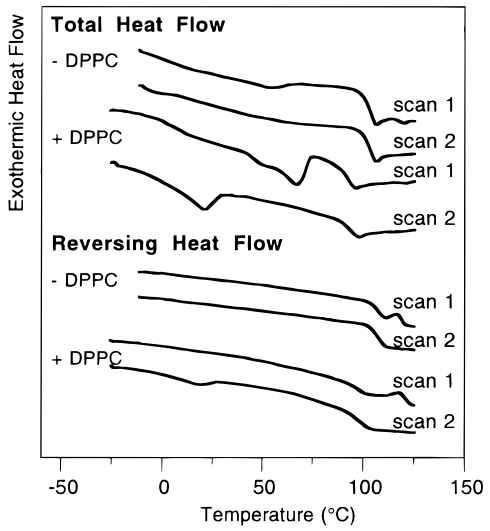


**Figure 5**—MTDSC scan 1 and 2 of freeze-dried DPPC liposomes with a medium containing 10% trehalose, 1 mM EDTA, and 10 mM Hepes, pH 7.4. Cakes of the same medium without liposomes are shown as well. Carbohydrate/phospholipid ratio, 3 g/g; $q = 2$ °C/min; $T_a = 0.159$ °C, $p = 30$ s.

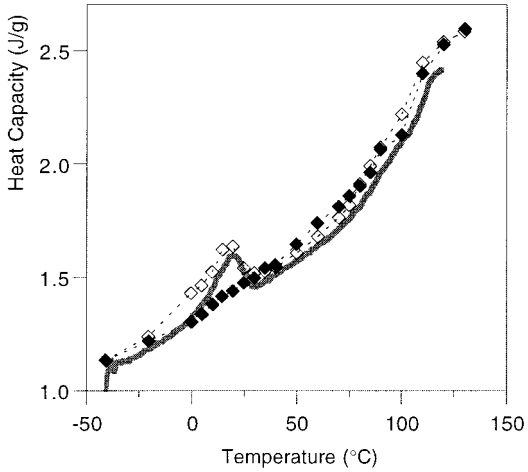


**Figure 6**—Heat capacity profile of DPPC liposomes freeze-dried in trehalose. $C_p$ values in scan 1 (- -◆•-) and scan 2 (- -◇•-) of quasi-isothermal measurements with $p = 100$ s and $T_a = 0.159$ °C. The $C_p$ was determined at 12–14 min after each change of the average temperature. Scan 3 (thick line) was performed with $q = 2$ °C/min, $p = 30$ s, and $T_a = 0.159$ °C.

variability of the residual water content in the different vials, and/or (3) the nonhomogeneity of the freeze-dried cakes. Changes in water content after closing the pans were typically less than 0.2% of the sample weight.

**Separation of Bilayer and Glass Transition**—In the experiments described above, cholesterol containing liposomes had been used which show no bilayer transition melting peak in the hydrated state. In the next experiments we used DPPC liposomes which have a clear melting peak in the hydrated state at 42 °C and trehalose as a lyoprotectant. As mentioned above, trehalose cakes lacked the pronounced baseline distortions frequently observed with other disaccharide cakes, which enabled us to monitor differences in the bilayer melting behavior in the first and second scan. Figure 5 shows the total and reversing heat flow in the first scan of a freeze-dried solution of 10% trehalose and 10 mM HEPES (pH 7.4) with and without liposomes. In the total heat flow of the first scan of freeze-dried trehalose with liposomes, an endothermic process is observed between 42 ± 2 and 73 ± 3 °C (average ± SD, $n = 8$), which is associated with the presence of phospholipids. A complete separation of the bilayer melting endotherm from the heat capacity changes in the reversing heat flow was obtained.

In the second scan major changes were observed in the liposome containing samples. The bilayer melting peak had shifted to lower temperatures and part of this signal now also appeared in the reversing heat flow. These findings agree well with other observations described in the literature.[17,18] The shift in bilayer transition temperature after a heating/cooling cycle of freeze-dried, lyoprotected liposomes has been ascribed to an enhanced interaction between the phospholipid and trehalose molecules.[17,18,27] From the presented data it is not clear yet at which temperature this change in interaction occurs and whether it results in a heat flow signal. This phenomenon will be further investigated in a different study.[28]

The appearance of the endothermic peak in the reversing heat flow was unexpected. The scanning rate and temperature modulation applied in the first and second scans were identical. In addition, the melting peak in the second scan had no particularly sharp appearance, which could have resulted in distortion of the sinusoidal shape of the modulated heat flow. To rule out artifacts originating from nonequilibrium conditions in the freeze-dried material during these scans, we subjected an identical sample to two subsequent quasi-isothermal heating scans in which the sample temperature was stepwise increased. In each step the average temperature was maintained constant for 14 min, while the temperature was modulated with $p = 100$ s and $T_a = 0.159$ °C. As demonstrated in Figure 2, these settings resulted in steady-state conditions in the freeze-dried cake. The heat capacity was determined from the data collected in the last 2 min of each step. In a third scan the same conditions were applied as described for Figure 5.

The heat capacity profiles of the first and second scan obtained under validated steady-state conditions as shown in Figure 6 are similar to the reversing heat flow curves obtained in the first two scans (Figure 5). In both experiments, no bilayer melting peak was observed in the first scan, whereas in the second scan similar increases in apparent heat capacity appeared around 15 °C. This is confirmed by the heat capacity profile obtained in a third scan of the same sample, using identical conditions as applied for Figure 5. This profile coincides with the quasi-isothermal curve of the second scan. In conclusion, the increase in apparent heat capacity which is associated with the bilayer transition in annealed, lyoprotected liposomes is not an artifact caused by nonequilibrium conditions. Thus, these results indicate that the melting characteristics of the bilayer have been changed by the annealing process, possibly by the enhanced interaction between the carbohydrate and the phospholipids in the annealed state. However, at this time we do not know exactly how this results in the apparent increase in amplitude of the modulated heat flow.

Interestingly, the absolute heat capacity values obtained with $q = 2$ °C/min, $p = 30$ s, and $T_a = 0.159$ °C (heating only conditions) are the same as measured under steady-state conditions. In contrast, the quasi-isothermal measurements with $p = 30$ s and $T_a = 0.159$ °C (heating–cooling conditions) did not result in steady-state conditions and gave an underestimation of the heat capacity (see Figure 2). Therefore, the average heating rate should also be considered when selecting steady-state measurement conditions.

**Separation of Overlapping $T_g$ and $T_m$**—The separation between the bilayer and glass transition signal may be particularly useful in cases where these two transitions coincide in the same temperature range (e.g. refs 17 and 29). To demonstrate this, DPPC liposomes in a 10% glucose

**Table 1—Transition Temperatures of Carbohydrate Solutions after Freezing or for Freeze-Dried DPPC Liposomes with Carbohydrates in and outside the Vesicles[a]**

| | freeze-concentrate ($n$=3–4) | | | dry cake | | | |
|---|---|---|---|---|---|---|---|
| carbohydrate | $T_{g,onset}$ (°C) | $T_s$ (°C) | $T_{dev,onset}$ (°C) | %$H_2O$ | $T_{g,onset}$ (°C) | $T_m$ (°C) | shrinkage |
| glucose | –63 ± 1 | –44.8 ± 0.4 | –58.3 ± 0.6 | 2.5 ± 0.2 ($n$=4) | 17 ($n$=1) | 42[c] ($n$=1) | + |
| | | | | 0.2 ± 0.5[b] ($n$=4) | 41[b] ($n$=1) | 43[b,c] ($n$=1) | +[b] |
| trehalose | –48.6 ± 0.9 | –30.7 ± 0.3 | –41 ± 2 | 0.4 ± 0.3 ($n$=4) | 93 ± 2 ($n$=4) | 42 ± 2<br>56 ± 3[c] ($n$=8) | – |

[a] The average vesicle size was 0.1 $\mu$m and the carbohydrate/phospholipid ratio was 3 g/g. The carbohydrate concentration in the solutions and the liposome dispersion was 10% (w/v) and contained 1 mM EDTA and 10 mM Hepes, pH 7.4. No differences in transition temperatures were found in frozen samples with and without liposomes (data not shown). For analysis of the freeze-concentrate 25 $\mu$L samples were frozen in a DSC pan at a cooling rate of ca. 17 °C/min to –80 °C. Both the frozen and the dry samples were scanned with $q$ = 2 °C/min, $p$ = 30 s, and $T_a$ = 0.159 °C. Data are expressed as average ± SD %$H_2O$, residual water content; $T_{g,onset}$, onset temperature of glass transition; $T_{dev,onset}$, onset temperature of devitrification process; $T_m$, main bilayer transition; $T_s$, softening temperature. [b] After an additional drying step under vacuum over dry $P_2O_5$ for 3 weeks. [c] The bilayer melting peak consisted of two overlapping peaks.

solution were freeze-dried. Freeze-drying of the glucose samples at a product temperature of −40 °C resulted in moderate collapse of the cakes during the process and a high residual water content (Table 1). No such shrinkage is observed with freeze-dried disaccharide solutions, which will be explained on the basis of thermal analysis of the frozen samples in the last section. Some of the cakes were subjected to an additional drying protocol under vacuum over dry $P_2O_5$. This decreased the residual water content from 2.5% to approximately 0.2% (see Table 1). The thermograms of the DPPC/glucose cakes with high and low residual water content are presented in Figure 7, parts A and B, respectively. In the cakes with a high water content, the $T_{g,onset}$ is found at 17 °C, whereas drying increased the $T_{g,onset}$ to 41 °C. Interestingly, the onset temperature of the bilayer transition was around 40−41 °C in both cakes, which is close to its value in an aqueous dispersion (42 °C). These data agree well with the values for $T_m$ of DPPC−glucose mixtures reported in previous studies, in which no glass transition was detected.[19,20] The explanation for this low value for $T_m$ of freeze-dried DPPC−glucose samples as compared with, for example, the $T_m$ for DPPC−trehalose samples is probably related to the differences in $T_g$ of these lyoprotectants in relation to the temperature during freeze-drying. This issue is beyond the scope of this study and will be addressed elsewhere.[28] Despite the strong endothermic bilayer melting peak, the underlying glass transition in the cakes with a low water content could still be observed in the reversing heat flow. In the high water content sample (2.5%), part of the sharp melting endotherm was observed in the reversing heat flow. In this case, the sharp peak shape of the bilayer transition probably resulted in a distorted shape of the sinusoidal heat flow modulation. Therefore, more temperature modulations in the temperature range of this transition may prevent such incomplete separation of the heat flow signals.

**MTDSC Analysis of Frozen Carbohydrate Solutions**—Finally, we demonstrate the value of MTDSC in analyzing frozen carbohydrate solutions to select optimal freeze-drying conditions. The collapse of the glucose cakes can be explained by transitions which take place in the frozen samples (e.g., refs 30 and 31). Figure 8 shows the heating curves of frozen solutions containing 10% glucose or 10% trehalose after quick freezing in DSC pans (15−18 °C/min).

Two transitions are observed in the reversing heat flow of both samples. The transition at the lower temperature is ascribed to a glass transition in the freeze-concentrate. The $T_{g,onset}$ in quickly frozen, nonannealed samples was −63 ± 1 °C (average ± SD $n$ = 3) and −48.6 ± 0.9 °C ($n$ = 4) for the glucose and trehalose solution, respectively (see

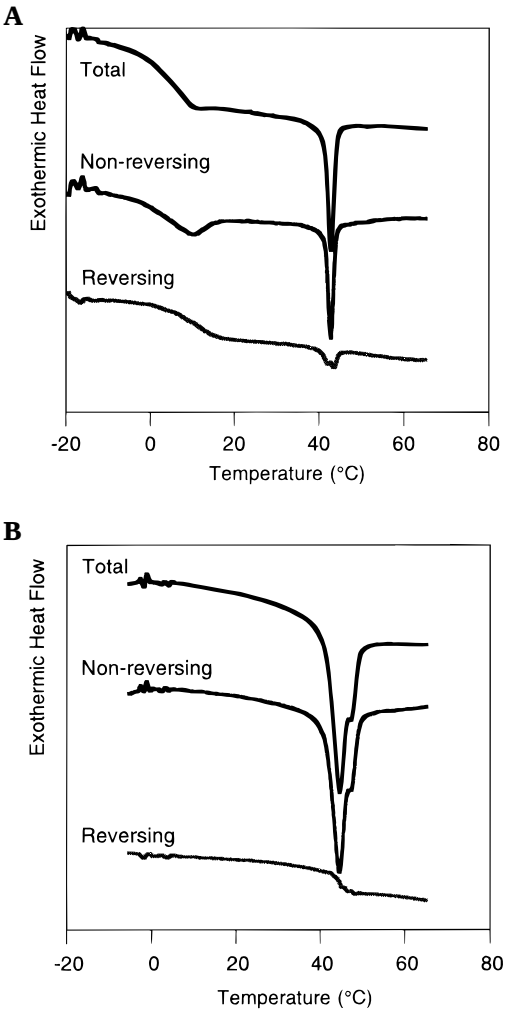


**Figure 7**—MTDSC scan 1 and 2 of freeze-dried DPPC liposomes with an extraliposomal medium containing 10% glucose and 10 mM Hepes, pH 7.4. The values of the residual water content of the cakes were 2.5 ± 0.2% (A) and 0.2 ± 0.5% (B). Carbohydrate/phospholipid ratio, 3 g/g; $q$ = 2 °C/min; $T_a$ = 0.159 °C; $p$ = 30 s.

Table 1). The second transition was found at −44.8 ± 0.4 °C (glucose) and −33.5 ± 0.5 °C (trehalose) and is here referred to as $T_s$ ("softening" temperature[31]). This transition is considered a critical parameter for the freeze-drying process. Only when the product temperature is maintained below this temperature will collapse be prevented after removal of the ice by sublimation. However, drying at temperatures above $T_s$ results in softening and collapse of

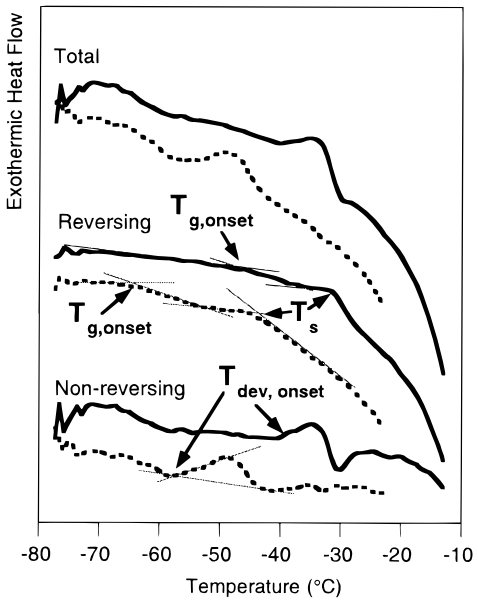


**Figure 8**—MTDSC scan of a frozen solution of 10% trehalose (—) and 10% glucose (- -) in 10 mM Hepes, pH 7.4, after freezing at ca. 17 °C/min to –80 °C. $q = 2$ °C/min, $T_a = 0.159$ °C, and $p = 30$ s.

the material and a reduced surface area. Therefore, drying can be incomplete, as was obviously the case for the glucose cakes which had been freeze-dried at −40 °C in the first, primary drying step. The nature of the transition at $T_s$ is still subject of discussion.[30−34] It has been ascribed to a glass transition ($T_{g'}$), to the onset melting of ice crystals ($T_{m,ice}$), or to a combination of both. MTDSC shows that this transition is accompanied by an increase in heat capacity.

In the nonreversing heat flow an exothermic peak can be discerned both for the glucose- and trehalose-containing system. This exotherm can be ascribed to (partial) devitrification of water present in the freeze-concentrate (e.g., refs 32 and 35). Although the implications of these three processes (glass transition, devitrification, and "softening" transition) for the preservation of the integrity of liposomes during the freezing and drying process are still unknown, it is clear that MTDSC provides insights into physical processes occurring at temperatures relevant during freeze-drying that could not be obtained by conventional DSC. MTDSC should therefore be able to further rationalize freeze-drying conditions for liposomes.

In summary, we demonstrated the potential of MTDSC for the analysis of freeze-dried and frozen phospholipid-carbohydrate mixtures. Separation of the glass transition related heat flow from other thermal events was achieved. In samples with overlapping thermal events, in which detection of the glass transition would be problematic with conventional DSC, MTDSC showed a clear glass transition in the reversing heat flow. We conclude that a validated MTDSC analysis provides valuable data to characterize freeze-dried, lyoprotected liposomes and can help to define optimal freeze-drying and storage conditions by rationale.

## References and Notes


1. Franks, F.; Van Den Berg, C. In *Topics in Pharmaceutical sciences*, Medpharm Scientific Publishers: Stuttgart, 1992; pp 233−240.
2. Friede, M., Van Regenmortel, M. H. V.; Schuber, F. *Am. Biotechnol. Lab.* **1993**, *211*, 117−122.
3. Te Booy, M. P. W. M.; De Ruiter, R. A.; De Meere, A. L. J. *Pharm. Res.* **1992**, *9*, 109−114.
4. Skrabanja, A. T. P.; De Meere, A. L. J.; De Ruiter, R. A.; Van Den Oetelaar, P. J. M. *Technology/Applications* **1994**, *48*, 311−317.
5. Townsend, M. W.; DeLuca, P. P. *J. Parent. Sci. Technol.* **1988**, *42*, 190−199.
6. Izutsu, K.; Yoshioka, S.; Takeda, Y. *Int. J. Pharm.* **1991**, *71*, 137−146.
7. Van den Berg, C. *Carbohydr. Netherlands* **1992**, *8*, 23−25.
8. Roos, Y.; Karel, M. *Food Technol.* **1991**, *12*, 66−107.
9. Levine, H.; Slade, L. *J. Chem. Soc., Faraday Trans. 1* **1988**, *84*, 2619−2633.
10. Wunderlich, B.; Jin, Y.; Boller, A. *Thermochim. Acta* **1994**, *238*, 277−293.
11. Reading, M., Elliot, D.; Hill, V. L. *J. Therm. Anal.* **1993**, *40*, 949−955.
12. Reading, M. *Trends Polym. Sci.* **1993**, *1*, 248−253.
13. Reading, M.; Luget, A.; Wilson, R. *Thermochim. Acta* **1994**, *238*, 295−307.
14. Gill, P. S.; Saurbrunn, S. R.; Reading, M. *J. Therm. Anal.* **1993**, *40*,.
15. Coleman, N. J.; Craig, D. Q. M. *Int. J. Pharm.* **1996**, *135*, 13−29.
16. Sun, W. Q.; Leopold, A. C.; Crowe, L. M.; Crowe, J. H. *Biophys. J.* **1996**, *70*, 1769−1776.
17. Mobley, W. C.; Schreier, H. *J. Controlled Release* **1994**, *31*, 73−87.
18. Crowe, L. M.; Crowe, J. H. *Biochim. Biophys. Acta* **1988**, *946*, 193−201.
19. Tanaka, K.; Takeda, T.; Fuji, K.; Miyama, K. *Chem. Pharm. Bull.* **1992**, *40*, 1−5.
20. Suzuki, T.; Komatsu, H.; Miyajima, K. *Biochim. Biophys. Acta* **1996**, *1278*, 176−182.
21. Zuidam, N. J.; Crommelin, D. J. A. *J. Pharm. Sci.* **1995**, *84*, 1113−1119.
22. Beijnen, J. H.; Van der Houwen, O. A. G. J.; Underberg, W. J. M. *Int. J. Pharm.* **1986**, *32*, 123−131.
23. Van Winden, E. C. A.; Crommelin, D. J. A. *Eur. J. Pharm. Biopharm.* **1997**, *43*, 295−307.
24. Haran, G.; Cohen, R.; Bar, L. K.; Barenholz, Y. *Biochim. Biophys. Acta* **1993**, *1151*, 201−215.
25. Storm, G.; Van Bloois, L.; Brouwer, M.; Crommelin, D. J. A. *Biochim. Biophys. Acta* **1985**, *818*, 343−351.
26. Rouser, G., Fluscher, S.; Yamamoto, A. *Lipids* **1970**, *5*, 494−496.
27. Crowe, J. H.; Hoekstra, F. A.; Nguyen, K. H. N.; Crowe, L. M. *Biochim. Biophys. Acta* **1996**, *1280*, 187−196.
28. Van Winden, E. C. A.; Crommelin, D. J. A. Submitted.
29. Koster, K. L.; Webb, M. S.; Bryant, G.; Lynch, D. V. *Biochim. Biophys. Acta* **1994**, *1193*, 143−150.
30. Hatley, R. H. M.; Franks, F. *J. Therm. Anal.* **1991**, *37*, 1905−1914.
31. Shalaev, E. Y.; Franks, F. *Cryobiology* **1996**, *33*, 14−26.
32. Ablett, S.; Izzard, M. J.; Lillford, P. J. *J. Chem. Soc., Faraday Trans.* **1992**, *88*, 789−794.
33. Roos, Y.; Karel, M. *J. Food Sci.* **1991**, *56*, 266−267.
34. Sahagian, M. E.; Goff, H. D. *Thermochim. Acta* **1994**, *246*, 271−283.
35. Roos, Y.; Karel, M. *Int. J. Food Sci. Technol.* **1991**, *26*, 553−566.


## Acknowledgments


We wish to thank Pharmachemie B.V. for their financial support of this study and acknowledge the gifts of phospholipids by Lipoid GmbH.

JS970060B